Use of homoarginine to obtain attenuated cationic membrane lytic peptides

Kentarou Sakamoto, Misao Akishiba, Takahiro Iwata, Jan Vincent V. Arafiles, Miki Imanishi, Shiroh Futaki*

Institute for Chemical Research, Kyoto University, Uji, Kyoto 611-0011, Japan

Abstract

Our research group has been studying the design of intracellular delivery peptides based on cationic lytic peptides. By placing negatively charged amino acids on potentially hydrophobic faces of the peptides, membrane lytic activity is attenuated on the cell surface, whereas it recovers in endosomes, enabling cytosolic delivery of proteins including antibodies. These lytic peptides generally contain multiple lysines, facilitating cell surface interaction and membrane perturbation. This study evaluated the effect of lysine-to-homoarginine substitution using HAad as a model delivery peptide. The resulting peptide had a comparable or better delivery efficacy for Cre recombinase, antibodies, and the Cas9/sgRNA complex with one-quarter of the concentration of HAad, implying that a subtle structural difference can affect delivery activity.

Abbreviations

SE: standard error
ACAL: Atenuated cationic amphiphilic lytic
hArg, hR: homoarginine
Mtt: 4-methyltrityl
Alexa488: Alexa Fluor 488
CLSM: confocal laser scanning microscopy
LUV: large unilamellar vesicle
ANTS: 8-aminonaphthalene-1,3,6-trisulfonic acid
DPX: *p*-xylene-bis-pyridinium bromide
POPC: 1-palmitoyl-2-oleoyl-*sn*-glycero-3-phosphocholine
POPG: 1-palmitoyl-2-oleoyl-*sn*-glycero-3-phosphoglycerol
$[P/L]_{50}$: half-maximal effe ctive peptide/lipid ratios
$[\theta]_{222}$: molecular ellipticity at 222 nm
EGFP: enhanced green fluorescent protein
CRISPR: clustered regularly interspaced short palindromic repeat

To analyze and control cellular events, considerable research has focused on the development of intracellular delivery systems for bioactive proteins and peptides. The possible use of unnatural amino acids and functional moieties make this approach applicable to gene-transfection approaches that lead to protein expression in cells.[1, 2] These proteins and peptides are generally expected to reach the cytosol to achieve their functions. Endocytosis followed by transfer from the endosomes into the cytosol has been used as a practical delivery route (Fig. 1A). Here, preferential perturbation of endosomal membranes over the cell (plasma) membrane is needed to avoid cell damage during delivery. Endosome release must be accomplished before lysosomal degradation of the endosome-captured proteins. Numerous peptides and polymers have been reported to stimulate the release of endosome-trapped biomacromolecules.[3-8] However, there is considerable room to improve the efficacy.

Our research group uses attenuated cationic amphiphilic lytic (ACAL) peptides for intracellular protein/peptide delivery.[9-13] The membrane-rupturing effect of cationic lytic peptides is attenuated on cell surfaces by placing carboxy-bearing amino acid(s) such as glutamic acid on the potentially hydrophobic faces of the peptides. The peptides are also designed to retain net positive features that promote endocytic uptake of the peptides into endosomes. The pH inside endosomes is lower than on the cell surface, leading to protonation of the carboxy group. Enhancement of the interaction of the peptide with the endosomal membranes leads to rupture and subsequent endosomal escape of the endosome-trapped proteins. Based on this concept, we designed L17E (IWLTALKFLGKHAAKHEAKQQLSKL-amide)[9] and an improved version HAad (IWLTALKFLGKAAAKAXAKQXLSKL-amide, X = L-2-aminoadipic acid).[11] Simple mixing with these peptides in culture medium resulted in facile, efficient delivery of antibodies and other bioactive proteins into cells to exert their expected functions. The L17E and HAad sequences contain five lysine (Lys) residues that are responsible for the membrane-rupturing activities. Arginine (Arg) residues are often found in the sequences of cell-penetrating intracellular delivery peptides, including a basic peptide derived from human immunodeficiency virus type 1 Tat protein (TAT peptide: GRKKRRQRRRPPQ), and guanidino side chains play a crucial role in the cell-penetrating ability.[14, 15] Guanidino is a stronger base (pK_a, 12.5) than the amino moiety of Lys (pK_a, 10.5). This study analyzed the effect of altering the

structural features of the ACAL peptide HAad to resemble cell-penetrating peptides through an amino-to-guanidino substitution and observing the effect on the intracellular delivery activity.

Amino-to-guanidino [*i.e.*, Lys-to-homoarginine (hArg, hR)] conversion of HAad was conducted on peptide resin. The peptide chain was constructed using a Fmoc-Lys(Mtt) derivative (Mtt = 4-methyltrityl). After constructing the peptide chain, the Mtt groups were selectively cleaved by treatment with hexafluoroisopropanol/dichloromethane (1:4).[16] Then, amino-to-guanidino conversion was achieved by treatment with 1-amidinopyrazole hydrochloride in the presence of diisopropylethylamine.[17] The peptide resin was then treated with a mixture of trifluoroacetic acid and ethanedithiol (95:5). High-performance liquid chromatography purification yielded the guanidino version of HAad (HAad-hR) (Fig. 1B).

Prior to evaluating the cytosolic delivery activity of HAad-hR, the cytotoxicity of the peptide was assessed using the WST-8 assay of mitochondrial metabolic activity.[18] HAad (40 μM) is frequently used to obtain the maximum delivery effect with minimal cytotoxicity. It turned out that HAad-hR had greater cytotoxicity compared to HAad (Fig. S1), presumably due to the greater interaction of the guanidino moiety with lipid head groups, by forming two hydrogen bonds, compared to the amino moiety, which forms only one hydrogen bond; the peptide caused considerable cell death at concentrations exceeding 10 μM. Therefore, 40 μM HAad and 10 μM HAad-hR were used in this study.

Polydextran (10 kDa) fluorescently labeled with Alexa Fluor 488 (Alexa488-dextran) was used as a model macromolecule. HeLa cells were treated with Alexa488-dextran in the presence of 40 μM HAad or 10 μM HAad-hR for 1 h in α-minimum essential medium. The cytosolic distribution of Alexa488-dextran was analyzed using confocal laser scanning microscopy (CLSM) (Fig. 1C and D). Cells treated with Alexa488-dextran in the absence of peptides produced punctate Alexa488-dextran signals, implying that Alexa488-dextran mostly stays in the endosomes without being released into the cytosol. In comparison, ~75% of the cells treated with 40 μM HAad exhibited Alexa488-dextran signals spread throughout the cells, indicating cytosolic translocation of Alexa488-dextran. With HAad-hR-treatment (10 μM), ~70% of the cells exhibited cytosolic labeling by Alexa488-dextran. When the total cellular uptake of Alexa488-dextran was analyzed based on cellular fluorescence using flow cytometry, HAad and HAad-hR resulted in 2.2- and 3.7-fold uptake of dextran, respectively (Fig. 1E). These results imply that HAad-hR attains comparable or better cytosolic delivery relative to HAad. Serum proteins sometimes affect the efficacy of peptide-mediated intracellular delivery. Cytosolic distribution after incubation with 40 μM HAad and 10 μM HAad-hR in serum-containing medium was observed for 55% and 23% of the cells treated with the respective peptides, implying a larger effect for HAad-hR than for HAad (Fig. S2).

Another HAad analog in which a Lys in HAad was replaced by Arg (HAad-R) was also prepared. In marked contrast to the results for HAad-hR, 40 μM HAad-R yielded a marginal cytosolic distribution of Alexa488-dextran (Fig. S3). Considering that Arg and hArg have quite similar structures but with one methylene moiety missing in Arg compared with hArg, a subtle difference in the net hydrophobicity of the peptides may have a big effect on the delivery activity.

The mode of membrane rupture by HAad-hR was studied with a dye leakage assay using liposomes (large unilamellar vesicles (LUV), 100 nm in diameter) encapsulating 8-aminonaphthalene-1,3,6-trisulfonic acid (ANTS) as a fluorophore and *p*-xylene-bis-pyridinium bromide (DPX) as a quencher (Fig. 2A, Table 1).[9, 11] Membrane perturbation by the peptide releases ANTS and DPX from the liposomes, followed by eventual recovery of ANTS fluorescence. The major lipid components of cell membranes are zwitterionic, neutral phospholipids, whereas those of endosomal membranes are neutral and negatively charged phospholipids, including bis(monoacylglycero)phosphate.[19] Therefore, 1-palmitoyl-2-oleoyl-*sn*-glycero-3-phosphocholine (POPC) and POPC/1-palmitoyl-2-oleoyl-*sn*-glycero-3-phosphoglycerol (POPG) (3:1) liposomes were used as cell and endosomal membrane models, respectively. The leakage of peptides at neutral (7.4) and acidic (5.0) pH was used to analyze peptide effects at extracellular and intra-endosomal pH levels, respectively. As reported, little leakage was induced by HAad from POPC liposomes at pH 7.4 or 5.0. However, there was marked dye leakage from POPC/POPG liposomes with lower peptide concentration at pH 5.0 than at pH 7.4 (Table 1), implying that HAad preferentially perturbs endosomal membranes over cell membranes. With HAad-hR, the effect of pH and lipid composition on dye leakage was smaller than that of the original peptide HAad (Fig. 2A and Table 1). HAad-hR caused greater perturbation of POPC membranes than did HAad. Marked leakage was observed at a peptide/lipid ratio > 0.01. HAad-hR caused less leakage from POPC/POPG liposomes at pH 5.0, but more at pH 7.4.

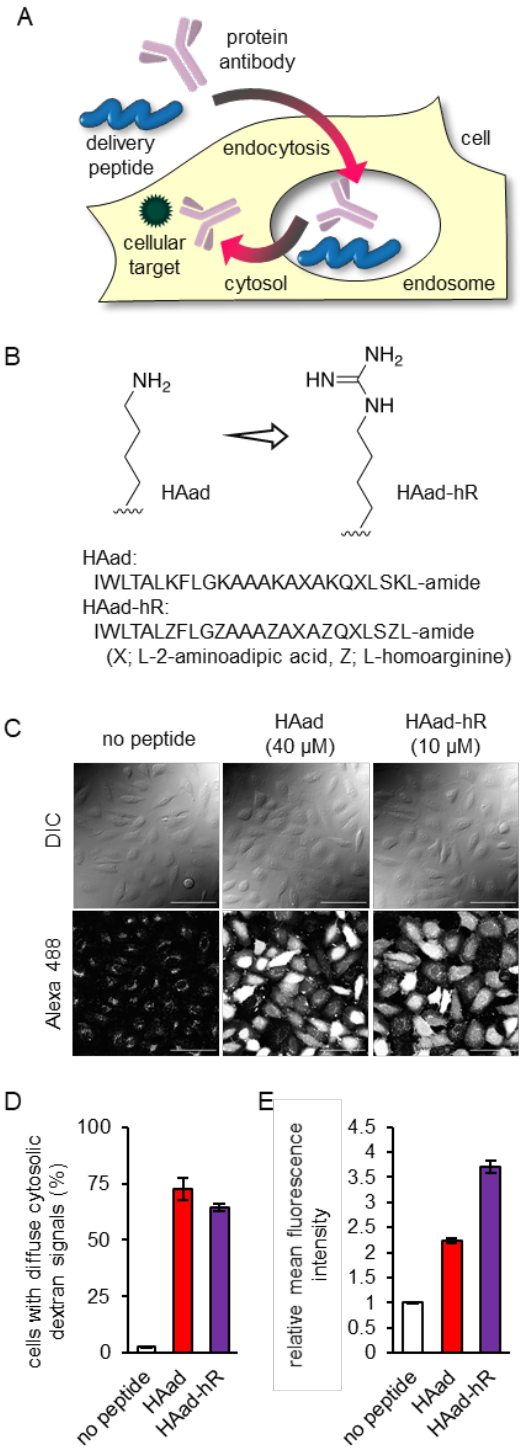

Figure 1. Replacement of lysine (Lys) in HAad with homoarginine (hArg, hR) yielded the cytosolic delivery peptide HAad-hR with an increased membrane interaction ability. (A) A general strategy for delivering bioactive proteins including antibodies via endocytic uptake followed by cytosolic release. (B) Schematic representation of the Lys-to-hArg conversion and the amino acid sequences of the HAad and HAad-hR peptides. (C) Cytosolic distribution of Alexa488-dextran (10 kDa) after treatment with 40 μM HAad and 10 μM HAad-hR for 1 h. Scale bar, 100 μm. (D) Percentages of cells with diffuse cytosolic labeling with Alexa488-dextran in (C). (E) Total cellular uptake of Alexa488-dextran after treatment with 40 μM HAad and 10 μM HAad-hR for 1 h (flow cytometry analysis). Results are presented as the mean ± standard error (SE, n = 3).

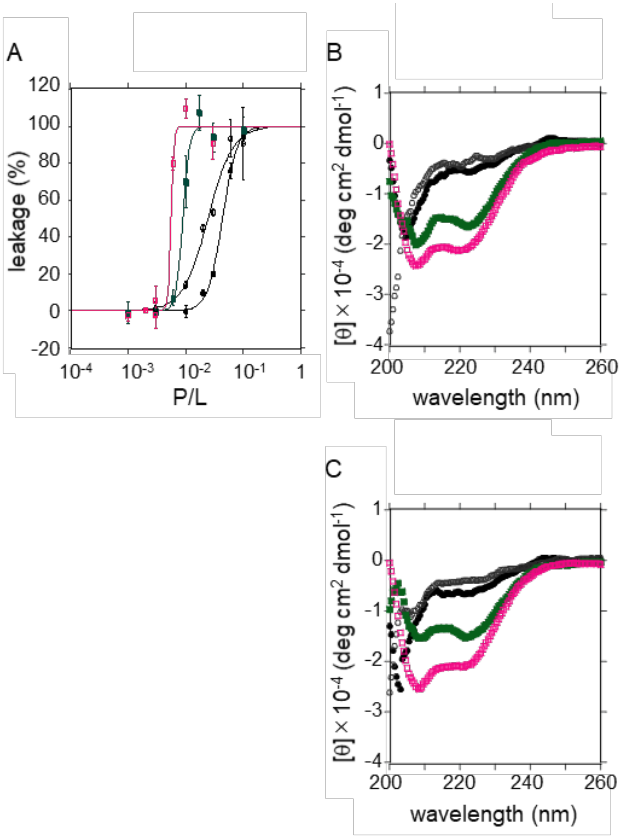

Figure 2. (A) Liposomal dye leakage upon treatment with HAad-hR, and (B) circular dichroism (CD) spectra of HAad-hR and (C) CD spectra of HAad-R in the presence of liposomes. Open magenta square, POPC/POPG (3:1) LUV at pH 5.0; filled green square, POPC/POPG (3:1) LUV at pH 7.4; open circle, POPC LUV at pH 5.0; filled circle, POPC LUV at pH 7.4.

Table 1. Half-maximal effective peptide/lipid ratios ($[P/L]_{50}$) to yield leakage for POPC/POPG and POPC LUVs by HAard-hR and HAad

	POPC/POPG		POPC only	
	pH 5.0	pH 7.4	pH 5.0	pH 7.4
HAad-hR	0.0056	0.0089	0.024	0.044
HAad	0.0023	0.040	N/D	N/D

Table 2. Molar ellipticity at 222 nm ($[\theta]_{222}$) ($\times 10^3$ deg cm^2 dmol^{-1}) of HAad-hR and HAad in the presence of PC/PG and PC LUVs

	POPC/POPG		POPC only	
	pH 5.0	pH 7.4	pH 5.0	pH 7.4
HAad-hR	–21	–15	–4.1	–6.5
HAad	–27	–8.0	–2.5	–2.7

The helical content as analyzed by the circular dichroism spectra of HAad, based on molar ellipticity at 222 nm, in the presence of POPC and POPC/POPG liposomes at pH 5.0 and 7.4, correlated well with the leakage activity of the peptide (Table 2). The absolute values of $[\theta]_{222}$ were in the order POPC/POPG at pH 5.0 >> POPC/POPG at pH 7.4 > POPC at pH 5.0 and 7.4. Although a similar tendency was observed for HAad-hR, the absolute value of $[\theta]_{222}$ for this peptide in the presence of POPC/POPG at pH 5.0 ($[\theta]_{222}$ = -2.1×10^4 deg·cm^2/dmol) was smaller than that of HAad ($[\theta]_{222} = -2.7 \times 10^4$ deg·cm^2/dmol). The absolute value for HAad-hR in the presence of POPC/POPG at pH 7.4 ($[\theta]_{222} = -1.5 \times 10^4$ deg·cm^2/dmol) was larger than that for HAad ($[\theta]_{222} = -8.0 \times 10^3$ deg·cm^2/dmol) (Fig. 2B, Table 2). One possible explanation for the above differences in the mode of membrane destabilization between HAad and HAad-hR may be that amino-to-guanidino conversion enhances the peptide interaction with lipid heads, making the pH effect less evident. In HAad-hR, hArgs are less favorable for helical structure formation than are lysines in HAad. This could explain the reason why HAad forms a more canonical helical structure, which is more favorable for stable membrane pore formation/rupture.

We next compared the delivery activity of bioactive proteins using HAad with that using HAad-hR in terms of a Cre-loxP recombination assay system (Fig. 3A).[5] HeLa cells transfected with a loxP-reporter plasmid comprised of loxP-DsRed-STOP-loxP-EGFP were incubated with Cre recombinase (38 kDa, 5 or 10 μM) in the presence of 40 μM HAad or 10 μM HAad-hR. The cells originally expressed DsRed. Cytosolic delivery of Cre with the help of the peptides led to the elimination of the DsRed-encoding DNA segment between the loxP sites, and the cells starts to express EGFP. The efficacy of the cytosolic translocation of Cre was then analyzed using CLSM. In the presence of HAad-hR, 10 and 5 μM Cre produced a yield of 63% and 50%, respectively, of fluorescent-protein-expressing cells displaying EGFP signals, which had previously expressed DsRed (Fig. 3B and C). The ratio of conversion was comparable to that obtained from treatment with HAad. HAad-hR was also capable of delivering IgG into the cytosol. HeLa cells were treated with Alexa488-labeled IgG (Alexa488- IgG, 200 μg/mL) together with 40 μM HAad or 10 μM HAad-hR for 1 h (Fig. 3D and E). Although the percentages of cells exhibiting diffuse cytosolic Alexa488-IgG labeling were higher in the treatment with HAad, more intense Alexa488-IgG signals were seen in the HAad-hR-treated cells.

Delivery using the CRISPR/Cas9 system is a current focus in the drug-delivery field.[20] Although efficient intracellular Cas9 delivery using cationic lipids can be attained, the potential cytotoxicity associated with cationic lipids affects their application *in vivo*. Therefore, the applicability of HAad and HAad-hR to intracellular CRISPR/Cas9 delivery was examined. As a model, Cas9 (TrueCut Cas9 protein v2, Invitrogen) and single guide RNA (sgRNA; TrueGuide Synthetic sgRNA for human HPRT1, Invitrogen) were mixed in the presence of Cas9 Plus Reagent (Invitrogen) to form the Cas9/sgRNA complex (ribonucleoprotein, RNP), prior to incubation with cells in the presence of peptides (40 μM HAad or 10 μM HAad-hR) for 6 h in Opti-MEM I reduced serum medium (Invitrogen). The cells were washed and incubated for another 2 days in the presence of serum. The gene-editing efficacy was then analyzed with GeneArt Genomic Cleavage Detection Kit (Invitrogen) (Fig. 4 and S4) (for analyzing procedure in detail, see Supporting Information). In the absence of peptides, no 250-bp band corresponding to the products of a double-strand break was observed, indicating the absence of genome editing. The band was apparent in the presence of HAad-hR, implying successful gene editing. The calculated efficiency of gene modification was 22%. HAad also exhibited activity, but with a lower gene-modification efficiency of 16%. Although the efficacy was not comparable to that obtained with the commercial cationic transfection agent Lipofectamine CRISPRMAX (Invitrogen) (63%, Fig. S4), these results imply the potential applicability of HAad-hR for Cas9/sgRNA delivery.

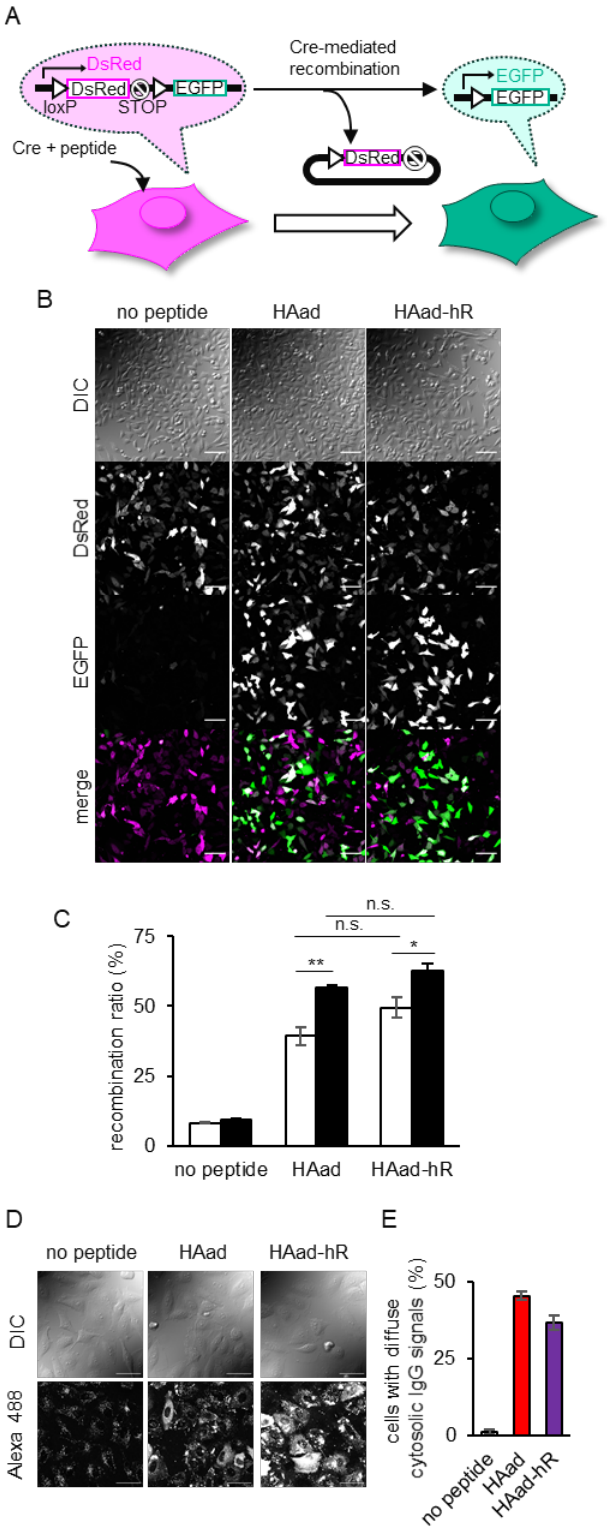

Figure 3. (A) Schematic representation of the Cre-loxP recombination assay system. (B) EGFP expression after treatment with 10 μM Cre in the presence of 40 μM HAad and 10 μM HAad-hR. Scale bar, 100 μm. (C) EGFP-positive cells (%) in loxP reporter-transfected cells. Open and filled columns represent the use of 5 and 10 μM Cre, respectively. Results are presented as the mean ± SE (n = 3). ** $p < 0.01$, * $p < 0.05$, n.s.: not significantly different based on Tukey–Kramer's honestly significant difference test. (D) Delivery of Alexa488-IgG (200 μg/mL) in the presence of 40 μM HAad and 10 μM HAad-hR (incubation, 1 h). Scale bar, 50 μm. (E) Percentages of cells in (D) with cytosolic IgG-Alexa signals.

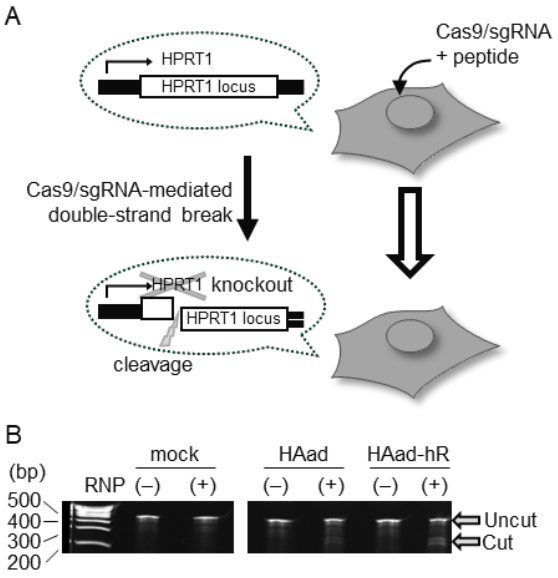

Figure 4. Peptide-mediated delivery of the Cas9/sgRNA complex. (A) Schematic illustration of Cas9/sgRNA-mediated endogenous gene knockout. HeLa cells were treated with a complex of Cas9 protein/sgRNA (human HPRT1) and Cas9 Plus Reagent in the presence of 40 μM HAad or 10 μM HAad-hR for 6 h. HPRT1 knockout was analyzed using GeneArt Genomic Cleavage Detection Kit. (B) Gene knockout was analyzed via non-denaturing polyacrylamide gel electrophoresis. A double-strand break in the target sequence was attained in HAad- and HAad-hR-treated cells.

In summary, the conversion of Lys to hArg in HAad altered the modes of membrane interaction and perturbation. Despite this, HAad-hR retained a delivery efficacy comparable to that of HAad. HAad-hR shares structural features with cell-penetrating peptides bearing a guanidino group on the HAad platform. Using HAad-hR and the Cas9/sgRNA complex, a double-strand break at the target locus was successfully induced. Although further studies are needed, some of the differences observed might have come from the greater interaction of HAad-hR with phosphates in lipid heads and nucleic acids, which has been implied by the membrane interactions of Arg-rich cell-penetrating peptides and DNA-binding peptides/proteins. As exemplified with HAad-R, a subtle difference of one methylene moiety yields a considerable difference in delivery activity.

Acknowledgements
This work was supported by JSPS KAKENHI (Grant Numbers 18H04403 and 18H04017), and by JST CREST (Grant Number JPMJCR18H5). K.S. and M.A. are grateful for the JSPS Research Fellowship for Young Scientists.

Declaration of Interest
The authors declare no conflicts of interest associated with this manuscript.

Supplementary Material
Materials and Methods.

References

1. Allen, J.; Najjar, K.; Erazo-Oliveras, A.; Kondow-Mcconaghy, H. M.; Brock, D. J.; Graham, K.; Hager, E. C.; Marschall, A. L. J.; Dübel, S.; Juliano, R. L.; et al. Cytosolic Delivery of Macromolecules in Live Human Cells Using the Combined Endosomal Escape Activities of a Small Molecule and Cell Penetrating Peptides. *ACS Chem. Biol.* **2019**,*14* (12) 12, 2641–2651. https://doi.org/10.1021/acschembio.9b00585.
2. Pei, D.; Buyanova, M. Overcoming Endosomal Entrapment in Drug Delivery. *Bioconjug. Chem.* **2019**, *30* (2), 273–283. https://doi.org/10.1021/acs.bioconjchem.8b00778.
3. Futaki, S.; Arafiles, J. V. V.; Hirose, H. Peptide-Assisted Intracellular Delivery of Biomacromolecules. *Chem. Lett.* **2020**, *49* (9), 1088–1094. https://doi.org/10.1246/cl.200392.
4. El-Sayed, A.; Futaki, S.; Harashima, H. Delivery of Macromolecules Using Arginine-Rich Cell-Penetrating Peptides: Ways to Overcome Endosomal Entrapment. *AAPS J.* **2009**, *11* (1), 13–22. https://doi.org/10.1208/s12248-008-9071-9072.
5. Méndez-Ardoy, A.; Lostalé-Seijo, I.; Montenegro, J. Where in the Cell Is Our Cargo? Methods Currently Used to Study Intracellular Cytosolic Localisation. *ChemBioChem* **2019**, *20* (4), 488–498. https://doi.org/10.1002/cbic.201800390.
6. Guha, S.; Ghimire, J.; Wu, E.; Wimley, W. C. Mechanistic Landscape of Membrane-Permeabilizing Peptides. *Chem. Rev.* **2019**, *119* (9), 6040–6085. https://doi.org/10.1021/acs.chemrev.8b00520.
7. Li, W.; Nicol, F.; Szoka, F. C. GALA: A Designed Synthetic pH-Responsive Amphipathic Peptide with Applications in Drug and Gene Delivery. *Adv. Drug Deliv. Rev.* **2004**, 56 (7), 967–985. https://doi.org/10.1016/j.addr.2003.10.041.
8. Meyer, M.; Philipp, A.; Oskuee, R.; Schmidt, C.; Wagner, E. Breathing Life into Polycations: Functionalization with pH-Responsive Endosomolytic Peptides and Polyethylene Glycol Enables siRNA Delivery. *J. Am. Chem. Soc.* **2008**, *130* (11), 3272–3273. https://doi.org/10.1021/ja710344v.
9. Akishiba, M.; Takeuchi, T.; Kawaguchi, Y.; Sakamoto, K.; Yu, H.-H.; Nakase, I.; Takatani-Nakase, T.; Madani, F.; Gräslund, A.; Futaki, S. Cytosolic Antibody Delivery by Lipid-Sensitive Endosomolytic Peptide. *Nat. Chem.* **2017**, *9* (8), 751–761. https://doi.org/10.1038/NCHEM.2779.
10. Tamemoto, N.; Akishiba, M.; Sakamoto, K.; Kawano, K.; Noguchi, H.; Futaki, S. Rational Design Principles of Attenuated Cationic Lytic Peptides for Intracellular Delivery of Biomacromolecules. *Mol. Pharm.* **2020**, *17* (6), 2175–2185. https://doi.org/10.1021/acs.molpharmaceut.0c00312.
11. Sakamoto, K.; Akishiba, M.; Iwata, T.; Murata, K.; Mizuno, S. Optimizing Charge Switching in Membrane Lytic Peptides for Endosomal Release of Biomacromolecules. *Angew. Chem. Int. Ed.* 2**020**, *59* (45), 19990–19998. https://doi.org/10.1002/anie.202005887.
12. Yu, H. H.; Sakamoto, K.; Akishiba, M.; Tamemoto, N.; Hirose, H.; Nakase, I.; Imanishi, M.; Madani, F.; Gräslund, A.; Futaki, S. Conversion of Cationic Amphiphilic Lytic Peptides to Cell-Penetration Peptides. *Pept. Sci.* **2020**, *112* (1), e24144. https://doi.org/10.1002/pep2.24144.
13. Nomura, Y.; Sakamoto, K.; Akishiba, M.; Iwata, T.; Hirose, H.; Futaki, S. Improved Cytosolic Delivery of Macromolecules through Dimerization of Attenuated Lytic Peptides. *Bioorganic Med. Chem. Lett.* **2020**, *30* (17), 127362. https://doi.org/10.1016/j.bmcl.2020.127362.
14. Futaki, S.; Nakase, I. Cell-Surface Interactions on Arginine-Rich Cell-Penetrating Peptides Allow for Multiplex Modes of Internalization. *Acc. Chem. Res.* **2017**, *50* (10), 2449–2456. https://doi.org/10.1021/acs.accounts.7b00221.
15. Stanzl, E. G.; Trantow, B. M.; Vargas, J. R.; Wender, P. A. Fifteen Years of Cell-Penetrating, Guanidinium-Rich Molecular Transporters: Basic Science, Research Tools, and Clinical Applications. *Acc. Chem. Res.* **2013**, *46* (12), 2944–2954. https://doi.org/10.1021/ar4000554.
16. Kawaguchi, Y.; Takeuchi, T.; Kuwata, K.; Chiba, J.; Hatanaka, Y.; Nakase, I.; Futaki, S. Syndecan-4 Is a Receptor for Clathrin-Mediated Endocytosis of Arginine-Rich Cell-Penetrating Peptides. *Bioconjug. Chem.* **2016**, *27* (4), 1119–1130. https://doi.org/10.1021/acs.bioconjchem.6b00082.
17. Bernatowicz, M. S.; Wu, Y.; Matsueda. G. R. 1*H*-Pyrazole-1-Carboxamidine Hydrochloride an Attractive Reagent for Guanylation of Amines and Its Application to Peptide Synthesis. *J. Org. Chem.* **1992**, *57* (8), 2497–2502. https://doi.org/10.1021/jo00034a059
18. Ishiyama, M.; Miyazono, Y.; Sasamoto, K.; Ohkura, Y.; Ueno, K. A Highly Water-Soluble Disulfonated Tetrazolium Salt as a Chromogenic Indicator for NADH as Well as Cell Viability. *Talanta* **1997**, *44* (7), 1299–1305. https://doi.org/10.1016/S0039-9140(97)00017-9.
19. Matsuo, H.; Chevallier, J.; Mayran, N.; Le Blanc, I.; Ferguson, C.; Fauré, J.; Blanc, N. S.; Matile, S.; Dubochet, J.; Sadoul, R.; Parton, R.G.; Vilbois, F.; Gruenberg, J. Role of LBPA and Alix in Multivesicular Liposome Formation and Endosome Organization. *Science* **2004**, *303* (5657), 531–534. https://doi.org/10.1126/science.1092425.
20. Dowdy, S. F. Overcoming Cellular Barriers for RNA Therapeutics. *Nat. Biotechnol.* **2017**, *35* (3), 222–229. https://doi.org/10.1038/nbt.3802.

Graphical Abstract